

**Ubiquity of linear resistivity at intermediate temperature in bad metals**

G. R. Boyd

*Department of Physics, Georgetown University, Washington, DC 20057, USA*

V. Zlatić

*Institute of Physics, Zagreb POB 304, Croatia and Department of Physics, Georgetown University, Washington, DC 20057, USA*

J. K. Freericks

*Department of Physics, Georgetown University, Washington, DC 20057, USA*

(Received 10 April 2014; revised manuscript received 29 October 2014; published 20 February 2015)

Bad metals display transport behavior that differs from what is commonly seen in ordinary metals. One of the most significant differences is a resistivity that is linear in temperature and rises to well above the Ioffe-Regel limit (where the mean-free path is equal to the lattice spacing). Using an exact Kubo formula, we show that a linear resistivity naturally occurs for many systems when they are in an incoherent intermediate-temperature state. First, we provide a simple analytic model to give intuition for this phenomenology. Then, we verify the analytic arguments with numerical calculations for a simplified version of the Hubbard model which is solved with dynamical mean-field theory. Similar features have also been seen in Hubbard models, where they can begin at even lower temperatures due to the formation of resilient quasiparticles.

DOI: [10.1103/PhysRevB.91.075118](https://doi.org/10.1103/PhysRevB.91.075118)

PACS number(s): 71.10.Fd, 71.27.+a, 72.15.-v

**I. INTRODUCTION**

Transport properties of strongly correlated materials such as oxides in the families of vanadates [1], cobaltates [2], or cuprates [3], Kondo semiconductors such as FeSi [4,5], FeSb<sub>2</sub> [6], CeB<sub>6</sub> [7], or SmB<sub>6</sub> [8], and organic charge transfer salts [9] are poorly understood, despite an overwhelming amount of experimental work which established non-Fermi-liquid behavior for these systems [10,11]. In particular, a resistivity which rises linearly with temperature above the Mott-Ioffe-Regel limit [12] has become a hallmark for non-Fermi-liquid behavior [13]. One common feature of these vastly different materials is that they are formed by doping away from a Mott-Hubbard insulating state. Starting from this observation, and the ubiquity of quasilinear non-Fermi-liquid materials, we provide a simple explanation of the experimental data at moderate to high temperature.

We begin by deriving the transport coefficients using an analytic approach, in the spirit of Mahan and Sofo's work on the best thermoelectrics [14], where the optimization of transport properties was calculated based on a simplified ansatz for the (vertex-corrected) transport relaxation time which then allowed one to perform the optimization. Here, we work in a similar vein, but consider the temperature dependence of the resistivity based on a general discussion of the properties of the transport relaxation time for a strongly correlated metal. By modeling this simplest form for correlated transport, the results should hold for a wide range of materials, and thereby explain the ubiquity of the linear resistivity at intermediate temperature. In the second part, we substantiate the phenomenological results by calculating the resistivity of a nontrivial model of strongly correlated electrons propagating on a  $d$ -dimensional lattice. We use the Falicov-Kimball model which, like the Hubbard or periodic Anderson model, has a gap in the excitation spectrum and, unlike these other models, admits an exact solution for the resistivity at arbitrary doping and temperature.

**II. MODEL-INDEPENDENT PHENOMENOLOGY**

Our starting point is the Kubo formula for the conductivity which reads [15]

$$\sigma_{dc}(T) = \sigma_0 \sum_{\sigma} \int d\omega \left[ -\frac{df(\omega)}{d\omega} \right] \tau_{\sigma}(\omega), \quad (1)$$

where  $\sigma_0$  is a material-specific constant with units of conductivity, and  $[-df(\omega)/d\omega]$  is the derivative of the Fermi function that is sharply peaked around the chemical potential  $\mu$ , so that the integral is cut off outside the Fermi window  $|\omega| \geq k_B T$ . The summation is over the spin states  $\sigma$ , and  $\tau_{\sigma}(\omega)$  is the exact transport relaxation time which includes the velocity factors, averaged over the Fermi surface, and all the effects of vertex corrections, if present. We set  $k_B = \hbar = 1$  and measure all energies with respect to  $\mu$ .

Since  $\tau_{\sigma}(\omega)$  is non-negative and vanishes for energies outside the band, it must have at least one maximum within the band. In a Fermi liquid,  $\tau_{\sigma}(\omega)$  diverges as  $T \rightarrow 0$  and  $\omega \rightarrow 0$ , and the resistivity,  $\rho(T) = 1/\sigma_{dc}(T)$ , follows a  $T^2$  law at low temperature. If there is residual scattering, due to disorder for example, then the divergence gets cut off and the Fermi-liquid form no longer holds. In a pure strongly correlated metal, for temperatures *above* the low-temperature coherence scale, the transport relaxation time typically has two maxima, located in the upper and the lower Hubbard bands, and neither the shape nor the position of these broad maxima, relative to  $\mu(T)$ , change appreciably with temperature. The transport relaxation time of the Hubbard model, Falicov-Kimball model, Anderson model, and other effective models of strong correlations exhibits these features. Since the chemical potential of a strongly correlated metal is within one of the two Hubbard bands, we calculate the resistivity focusing on  $\tau_{\sigma}(\omega)$  with just a single broad maximum at  $\omega_0$ , neglecting the excitations across the gap.

The conductivity given by Eq. (1) crucially depends on the overlap between  $(-df/d\omega)$  and  $\tau_\sigma(\omega)$ , i.e., on temperature and doping. Temperature broadens the Fermi window where the integrand is appreciable, while doping changes the number of carriers, so that  $\mu$  gets shifted with respect to  $\omega_0$ . The value and the shape of  $\tau_\sigma(\omega)$  around  $\omega_0$  can also be doping dependent.

To estimate the resistivity, we expand  $\tau_\sigma(\omega)$  around its maximum at  $\omega_0$ ,

$$\tau_\sigma(\omega) \approx \tau_0 - \tau_1(\omega - \omega_0)^2, \quad (2)$$

where  $\tau_0 = \tau_\sigma(\omega_0)$ ,  $\tau_1 = -d^2\tau_\sigma(\omega)/2d\omega^2|_{\omega \rightarrow \omega_0}$ , and we use a simple model in which  $\tau_\sigma(\omega)$  is approximated by the parabolic form in Eq. (2) for  $\Lambda_- < \omega < \Lambda_+$  and  $\tau_\sigma(\omega) = 0$  otherwise; this form properly has a maximum, and shows linear behavior as one approaches the band edges, as expected for a three-dimensional material. The cutoffs  $\Lambda_\pm$  are obtained by setting  $\tau_\sigma(\omega) = 0$  in Eq. (2). This yields  $\Lambda_\pm = \omega_0 \pm x_0$ , where  $x_0^2 = \tau_0/\tau_1$  is inversely proportional to the curvature of  $\tau_\sigma(\omega)$  at  $\omega_0$  and  $x_0$  has dimensions of energy. Since the high-energy part of  $\tau_\sigma(\omega)$  does not contribute much to the conductivity,  $x_0 = \omega_0 - \Lambda_-$  often defines an effective bandwidth relevant for transport in a doped Mott insulator.

To evaluate the integral in Eq. (1), we introduce dimensionless variables,  $\nu = \omega/x_0$  and  $\tilde{T} = T/x_0$ , and write the relaxation time as  $\tau_\sigma(\nu)/\tau_0 = 1 - (\nu - \nu_0)^2$ , where  $\nu_0 = \omega_0/x_0$ . Integrating by parts, and using  $\tau_\sigma(\Lambda_-) = \tau_\sigma(\Lambda_+) = 0$ , yields

$$\sigma_{dc}(\tilde{T}) = 2\tau_0\sigma_0 \int_{\nu_0-1}^{\nu_0+1} d\nu f(\nu) \frac{d\tau(\nu)}{d\nu}, \quad (3)$$

where  $f(\nu) = 1/[1 + \exp(\nu/\tilde{T})]$ ,  $d\tau_a/d\nu = -2(\nu - \nu_0)$ , and we took the spin degeneracy into account. The integrand is a regular function and the numerical evaluation is straightforward. The renormalized resistivity,  $\rho(\tilde{T})/\rho_0$ , where  $\rho_0 = 1/(\sigma_0\tau_0)$ , is shown in Fig. 1(b) for several characteristic values of  $\nu_0$ . Figure 1(a) shows  $\tau_\sigma(\nu)/\tau_0$  used for each of the resistivity curves. The data indicate three types of behavior, depending on the relative position of  $\mu$  and  $\omega_0$ . Here,  $\mu$  is fixed as a function of  $T$ , but, as seen below, fixing the density instead produces similar results.

For  $\nu_0 \geq 1$ , when the chemical potential is close to the band edge, the resistivity decreases rapidly as temperature increases from  $T = 0$ . At about  $T \simeq \omega_0/2$ , the resistivity drops to a minimum and then increases with temperature, assuming a linear form at about  $T \simeq \omega_0$ . Such a behavior is typical of lightly doped Mott insulators. For  $\nu_0 \leq 1$ , when the chemical potential is just above the band edge, the low-temperature resistivity is metallic. It starts from a finite value, at  $T = 0$ , and grows to a well-pronounced maximum, which is reduced and shifted to lower temperature as  $\nu_0$  is reduced. The minimum still occurs at about  $T \simeq \omega_0/2$  and, for  $T \geq \omega_0$ , the resistivity becomes a linear function in a broad temperature range. Such a behavior is typical of bad metals. For  $\nu_0 \ll 1$ , the chemical potential is close to the maximum of  $\tau_\sigma(\nu)$  and  $\rho(T)$  increases parabolically from its zero-temperature value, as found in dirty metals. At higher temperatures,  $T > \omega_0$ , there is a crossover to the linear behavior. According to this simple model, strongly correlated materials are classified into three distinct groups: lightly doped insulators characterized by a low-temperature

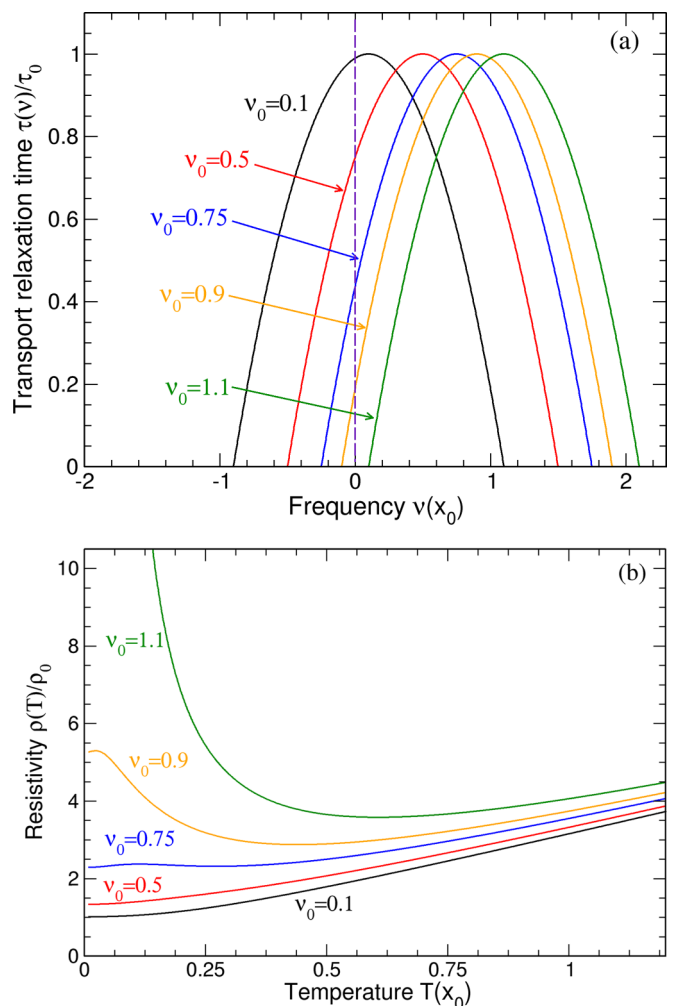


FIG. 1. (Color online) (a) Rescaled relaxation time  $\tilde{\tau}_\sigma(\nu)$  plotted as a function of rescaled frequency  $\nu = \omega/x_0$  relative to the chemical potential  $\mu$ , which is indicated by the vertical line at  $\nu = 0$ . (For definition of the scaling factors, see the text.) The different curves show  $\tau_\sigma(\nu)$  shifted with respect to  $\mu$  by  $\nu_0 = 0.1, 0.5, 0.75, 0.9$ , and  $1.1$ , respectively. (b) The rescaled resistivity obtained from Eq. (3) plotted as a function of rescaled temperature  $\tilde{T} = T/x_0$ . The different curves are obtained for  $\tilde{\tau}_\sigma(\nu)$  as defined in (a).

resistivity upturn, bad metals characterized by an extended range of quasilinear resistivity, and dirty metals characterized by a *constant plus*  $T^2$  behavior.

### III. MODEL-DEPENDENT EXAMPLE

The analytic approach is suggestive of the robustness of the linear resistivity for bad metals due to the general nature of  $\tau_\sigma(\omega)$ , but we want to go further to obtain similar results with a nontrivial microscopic model. We choose the spin-1/2 Falicov-Kimball model, which is closely related to the Hubbard model and leads to similar transport properties (above the coherence temperature of the Hubbard model). The question we primarily want to address is the following: to what extent can a model for strongly correlated electrons capture the phenomenology of non-Fermi-liquid electrical transport with a focus on the linear resistivity? The advantage of the

Falicov-Kimball model is that the dynamical mean-field theory (DMFT) provides an exact solution at arbitrary filling [16]. (There have been related studies on the Hubbard model using DMFT [17,18] exploring transport in bad metals as well.)

The spin-1/2 Falicov-Kimball Hamiltonian reads

$$H = -\frac{t^*}{2\sqrt{d}} \sum_{(i,j)\sigma} c_{i\sigma}^\dagger c_{j\sigma} + U \sum_{i\sigma} w_i c_{i\sigma}^\dagger c_{i\sigma}, \quad (4)$$

where  $c_{i\sigma}^\dagger$  ( $c_{i\sigma}$ ) is the mobile electron creation (annihilation) operator of spin  $\sigma$ , and  $w_i$  is 1 or 0 and represents the localized electron number operator at site  $i$ . (Each lattice site can only be occupied by a single localized electron because the on-site repulsion between the localized electrons of the opposite spin is assumed infinite.) The interaction of the conduction electrons with localized electrons is  $U$  and  $t^*$  is the hopping integral scaled so that we can properly take the  $d \rightarrow \infty$  limit [19]. We work on both a hypercubic and Bethe lattice using units where  $t^* = 1$ . We maintain the paramagnetic constraint,  $\rho_{c\sigma} = \rho_{c\bar{\sigma}} = \rho_c$ , by equating the conduction and localized densities. For hole doping, we have  $\rho_c = \rho_f = 1 - \delta \leq 1$ , where  $\delta$  is the concentration of the holes in the lower Hubbard band, while for electron doping,  $\rho_c = 1 + \delta \geq 1$ , where  $\delta$  is the concentration of electrons in the upper Hubbard band.

The model is solved using DMFT [20] in the infinite-dimensional limit  $d \rightarrow \infty$ , such that the self-energy  $\Sigma(\omega)$  is a functional of the local conduction electron Green's function,  $G_{loc}(\omega)$ , and the full lattice problem is equivalent to a single-site model with an electron coupled self-consistently to a time-dependent external field. Several reviews, whose notation we adopt, now exist both on DMFT generally [21] and on the exact DMFT for the Falicov-Kimball model [16]. We find  $\Sigma(\omega)$ ,  $G_{loc}(\omega)$ , and the local density of conduction states  $\rho_{loc}(\omega) = -\text{Im}G_{loc}(\omega)/\pi$  numerically using methods described elsewhere [22].

For  $\rho_c = 1$ ,  $\rho_{loc}(\omega)$  is symmetric and, for large enough  $U$ , we have a Mott insulator in which a filled lower Hubbard band is separated from an empty upper Hubbard band by a band gap with the chemical potential in the middle of the gap ( $U_c = \sqrt{2}$  for the hypercubic lattice and  $U_c = 2$  for the Bethe lattice). Away from half filling,  $\rho_{loc}(\omega)$  is asymmetric and for electron doping, which is the case we consider, the chemical potential is in the upper Hubbard band. Its distance from the lower band edge  $\Lambda_-$  is determined by charge conservation  $\delta = 2 \int d\omega f(\omega) \rho_{loc}(\omega) - 1$ .

For  $d \rightarrow \infty$ , the vertex corrections to the conductivity vanish [23] and explicit formulas can be found for the relaxation time. On the Bethe lattice, this yields [24]

$$\tau_\sigma(\omega) = \frac{1}{3\pi^2} \text{Im}^2[G_{loc}(\omega)] \left[ \frac{|G_{loc}(\omega)|^2 - 3}{|G_{loc}(\omega)|^2 - 1} \right], \quad (5)$$

while on the hypercubic lattice, we have [16]

$$\tau_\sigma(\omega) = \frac{1}{4\pi^2} \frac{\text{Im}G_{loc}(\omega)}{\text{Im}\Sigma(\omega)} + \frac{1}{2\pi^2} (1 - \text{Re}\{[\omega + \mu - \Sigma(\omega)]G_{loc}(\omega)\}). \quad (6)$$

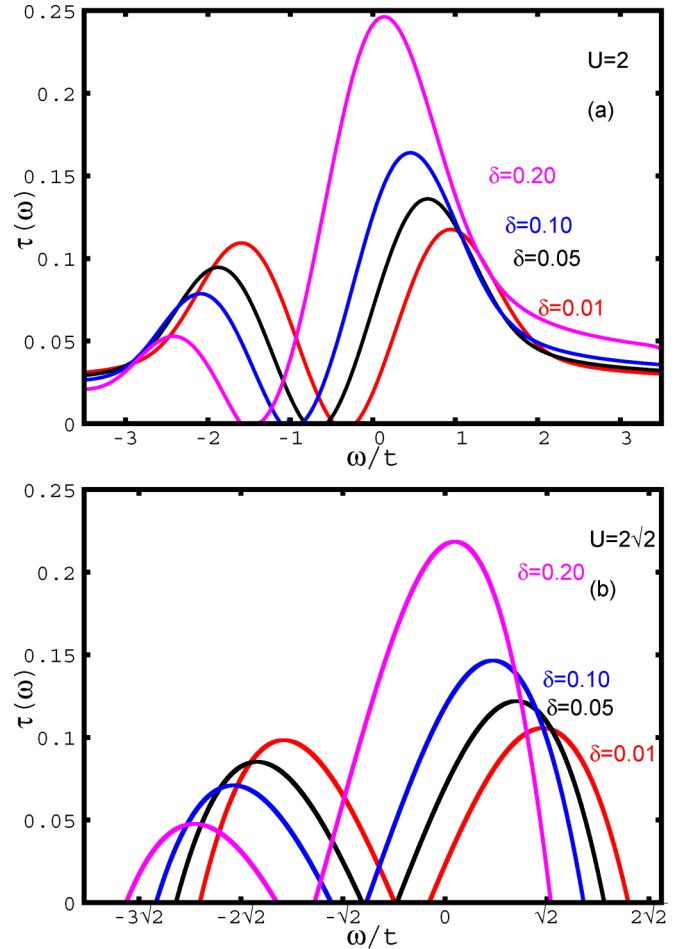


FIG. 2. (Color online) Transport lifetimes in the Falicov-Kimball model for (a)  $U = 2t^*$  on a hypercubic lattice and (b)  $U = 2\sqrt{2}t^*$  on the Bethe lattice.

For fixed  $\rho_f$ , the shape of  $\tau_\sigma(\omega)$  is independent of temperature. In a Fermi liquid, where one can approximate [15]  $\tau_\sigma(\omega) \simeq \text{Im}G_{loc}(\omega)/\text{Im}\Sigma(\omega)$  with  $\text{Im}\Sigma(\omega \rightarrow 0) \rightarrow 0$ , the relaxation time  $\tau_\sigma(\omega)$  diverges as  $\omega \rightarrow 0$ . In the Falicov-Kimball model, however,  $\text{Im}\Sigma(0)$  does not vanish and  $\tau_\sigma(0)$  remains finite. For large  $U$ , the width of the single-particle excitations exceeds their energy, leading to overdamped excitations rather than with quasiparticles, such that the Fermi-liquid description is not applicable.

The transport relaxation time of the Falicov-Kimball model due to such overdamped excitations, obtained for a fixed value of  $U$  and several values of  $\delta$ , is shown in Fig. 2. The left and right panel show the results for the hypercubic and Bethe lattice, respectively. Note the similarity to the inverse quadratic approximation used in the first part. The transport relaxation time vanishes below the band edge  $\Lambda_-$  and has a peak at the energy  $\omega_0$ , in the upper Hubbard band (for electron doping). As  $\delta$  increases,  $\omega_0$  and  $\Lambda_-$  decrease but the difference  $\omega_0 - \Lambda_-$  remains approximately constant. The resistivity obtained for the same set of parameters is shown in Fig. 3. The doping dependence of  $\rho(T)$  follows from the observation that  $\delta$  reduces  $\omega_0$  and that, for  $\Lambda_- < \mu < \omega_0$ , the Fermi window removes the contribution of the high-energy part of  $\tau_\sigma(\omega)$ .

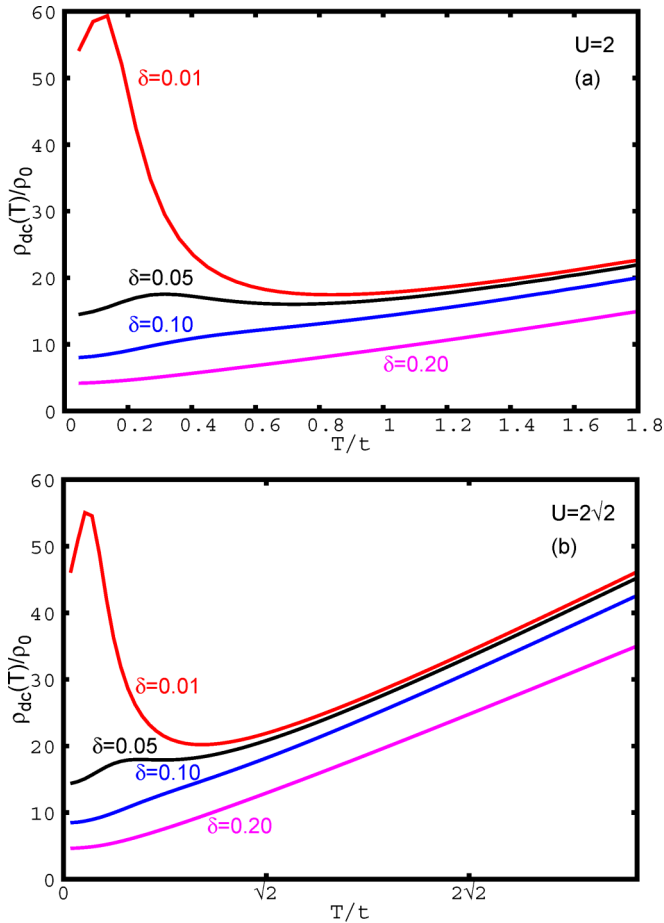


FIG. 3. (Color online) Resistivity for (a)  $U = 2t$  on the hypercubic lattice and (b)  $U = 2\sqrt{2}t$  on the Bethe lattice.

Close to half filling (very small  $\delta$ ), where  $\mu \simeq \Lambda_- \ll \omega_0$ , the resistivity exhibits a low-temperature peak, then drops to a minimum at about  $T \simeq \omega_0/2$  and, eventually, becomes a linear function of  $T$ , for  $T \geq \omega_0$ . An increase of  $\delta$  brings  $\omega_0$  closer to  $\mu$ , which reduces the resistivity maximum and brings the onset of the linear region to lower temperatures. For a sufficiently large  $\delta$ , the maximum is completely suppressed and the resistivity is a monotonically increasing function of temperature. For  $\delta \simeq 0.2$ , we find  $\omega_0 \simeq \mu$  and obtain a resistivity with a well-defined  $T^2$  term at the lowest temperatures. Note that the

crossover between different regimes can also be induced by pressure which modifies the hopping integrals and shifts  $\omega_0$  with respect to  $\mu$ .

#### IV. CONCLUSIONS

The results obtained for the Falicov-Kimball model are in complete agreement with the phenomenological theory presented in the first part of the paper. Hence, the analytic model is verified as providing the generic behavior of a doped Mott insulator at intermediate  $T$ . The central result of this paper is that the linear resistivity seen in strongly correlated materials at intermediate  $T$  is governed by the appearance of a maximum in  $\tau_\sigma(\omega)$  above the chemical potential. The slope of the linear resistivity does not vary much for a range of chemical potentials near the maximum, so the temperature dependence of  $\mu(T)$  does not change this behavior. In other correlated models such as the Hubbard model, the linear resistivity will disappear when  $T$  is reduced below the renormalized Fermi-liquid scale, but it appears that the resilient quasiparticle picture [25] allows the linear region to be brought down to even lower  $T$ 's than seen in the Falicov-Kimball model. In the very high- $T$  limit, where  $T$  is bigger than the bandwidth, general arguments [26] show that the resistivity is linear for the Bethe lattice, but saturates at a constant for the hypercubic lattice. Those results are complementary to the general linear resistivity here, found for temperatures much less than the bandwidth.

#### ACKNOWLEDGMENTS

J.K.F. and V.Z. were supported by the National Science Foundation under Grant No. DMR-1006605 and the Ministry of Science of Croatia under the bilateral agreement with the USA on the scientific and technological cooperation, Project No. 1/2014, for the data analysis. J.K.F. and G.R.B. were supported by the Department of Energy, Office of Basic Energy Sciences, under Grant No. DE-FG02-08ER46542 for the development of the numerical analysis and the development of the analytic model. The collaboration was supported the Department of Energy, Office of Basic Energy Sciences, Computational Materials and Chemical Sciences Network Grant No. DE-SC0007091. J.K.F. was also supported by the McDevitt bequest at Georgetown University.

- 
- [1] C. Urano, M. Nohara, S. Kondo, F. Sakai, H. Takagi, T. Shiraki, and T. Okubo, *Phys. Rev. Lett.* **85**, 1052 (2000).
  - [2] M. Kriener, C. Zobel, A. Reichl, J. Baier, M. Cwik, K. Berggold, H. Kierspel, O. Zabara, A. Freimuth, and T. Lorenz, *Phys. Rev. B* **69**, 094417 (2004).
  - [3] N. E. Hussey, K. Takenaka, and H. Takagi, *Philos. Mag.* **84**, 2847 (2004).
  - [4] N. Manyala, J. F. Di-Tusa, G. Aeppli, and A. P. Ramirez, *Nature (London)* **454**, 976 (2008).
  - [5] B. C. Sales, O. Delaire, M. A. McGuire, and A. F. May, *Phys. Rev. B* **83**, 125209 (2011).
  - [6] Q. Jie, R. Hu, E. Bozin, A. Llobet, I. Zaliznyak, C. Petrovic, and Q. Li, *Phys. Rev. B* **86**, 115121 (2012).
  - [7] S.-I. Kobayashi, M. Sera, M. Hiroi, N. Kobayashi, and S. Kunii, *J. Phys. Soc. Jpn.* **69**, 926 (2000).
  - [8] J. C. Cooley, M. C. Aronson, Z. Fisk, and P. C. Canfield, *Phys. Rev. Lett.* **74**, 1629 (1995).
  - [9] B. J. Powell and R. H. McKenzie, *Rep. Prog. Phys.* **74**, 056501 (2011).
  - [10] G. R. Stewart, *Rev. Mod. Phys.* **73**, 797 (2001).
  - [11] M. Imada, A. Fujimori, and Y. Tokura, *Rev. Mod. Phys.* **70**, 1039 (1998).

- [12] A. F. Ioffe and A. R. Regel, in *Progress in Semiconductors*, Vol. 4, edited by A. F. Gibson (Wiley, New York, 1960), p. 237.
- [13] H. v. Löhneysen, A. Rosch, M. Vojta, and P. Wölfle, *Rev. Mod. Phys.* **79**, 1015 (2007).
- [14] G. D. Mahan and J. O. Sofo, *Proc. Natl. Acad. Sci. USA* **93**, 7436 (1996).
- [15] G. D. Mahan, *Many-Particle Physics* (Plenum, New York, 1981).
- [16] J. K. Freericks and V. Zlatić, *Rev. Mod. Phys.* **75**, 1333 (2003).
- [17] W. Xu, K. Haule, and G. Kotliar, *Phys. Rev. Lett.* **111**, 036401 (2013).
- [18] J. Merino and R. H. McKenzie, *Phys. Rev. B* **61**, 7996 (2000).
- [19] W. Metzner and D. Vollhardt, *Phys. Rev. Lett.* **62**, 324 (1989).
- [20] U. Brandt and C. Mielsch, *Z. Phys. B* **75**, 365 (1989).
- [21] A. Georges, G. Kotliar, W. Krauth, and M. J. Rozenberg, *Rev. Mod. Phys.* **68**, 13 (1996).
- [22] M. Jarrell, *Phys. Rev. Lett.* **69**, 168 (1992).
- [23] V. Zlatić and B. Horvatić, *Solid State Commun.* **75**, 263 (1990).
- [24] A. V. Jura, D. O. Demchenko, and J. K. Freericks, *Phys. Rev. B* **69**, 165105 (2004).
- [25] X. Deng, J. Mravlje, R. Žitko, M. Ferrero, G. Kotliar, and A. Georges, *Phys. Rev. Lett.* **110**, 086401 (2013).
- [26] G. Pálsson and G. Kotliar, *Phys. Rev. Lett.* **80**, 4775 (1998).